Iterative Space-Time Soft Interference Cancellation for UMTS-FDD Uplink*

David MOTTIER, Loïc BRUNEL

Mitsubishi Electric ITE, Telecommunication Laboratory
1, Allée de Beaulieu - CS 10806
35708 Rennes Cedex 7, France
{mottier,brunel}@tcl.ite.mee.com

January 9, 2003

Submission to IEEE Trans. on Vehicular Technology - Revision 1.0

Abstract

In this paper, two efficient pilot-aided iterative space-time interference cancellation receivers are studied in order to increase the uplink capacity of Universal Mobile Telecommunication System (UMTS) in Frequency Division Duplex (FDD) mode. Both iterative schemes use low complexity beamforming and path combining techniques associated to soft-input soft-output (SISO) decoding to mitigate the multiple access interference in space and time. The difference of the proposed techniques rely on the way they deal with unknown channels: The addition of a space-time channel estimation in each iteration on one hand and iterative adaptive beamforming and path combining on the other hand. Thanks to the iterative structure, the observation signal used for estimation or adaptation contains less interference from one iteration to the following and soft estimates of coded bits are available for data-aided estimation or adaptation. A detailed complexity analysis shows that renewing beamforming and path combining in each iteration without a

*Part of the material in this paper has been presented in the IST Mobile Communications Summit (IST-MCS'01), Barcelona, Spain, Sept. 2001, and in the IEEE Vehicular Technology Conference (VTC'01 Fall), Atlantic City, USA, Oct. 2001.

priori knowledge on the channel has no significant impact of the overall complexity of one iteration. Simulations of true UMTS-FDD uplink communications over a wideband directional channel model reveal that near-single user performance can be obtained for very high system loads, whereas more conventional receivers such as the interference canceller without beamforming and the two-dimensional Rake receiver fail in recovering the transmitted information.

Key Words: Beamforming, Multiuser Detection, Interference Cancellation, Iterative Techniques, Channel Estimation, Adaptive Space-Time Processing, W-CDMA, UMTS-FDD.

1 Introduction

The third generation (3G) of mobile cellular radio systems, i.e., the Universal Mobile Telecommunication System (UMTS), will allow transmission data rates up to 2 Mbit/s with an air interface based on Wideband Code Division Multiple Access (W-CDMA) [1]. In order to exploit the available paired and unpaired frequency bands of the spectral resource, both Frequency Division Duplex (FDD) and Time Division Duplex (TDD) are considered to deal with uplink and downlink communications. However, the FDD mode currently receives more attention from manufacturers as it should be used to launch 3G services.

To cope with the relatively low level of traffic and associated interference generated by 3G first subscribers, simple demodulation techniques, such as Rake receivers [17], will probably be employed in a first step. Subsequently, advanced receiver techniques will have to be implemented to face the expected increase of traffic and interference. Several interference mitigation techniques have been studied for W-CDMA Base Station (BS) receivers, where additional computational complexity is tolerable [15]. Due to the large size of spreading sequences available for UMTS-FDD (the spreading factor may be as

large as 256) and the existence of a scrambling code with length $2^{25}-1$, multi-user detection techniques based on matrix inversion require too much computational complexity. In contrast, techniques based on Interference Cancellation (IC) [22] seem appropriate to mitigate intra-cell interference with a reasonable complexity increase. The interference on a given user is rebuilt from a bank of Rake receivers and subtracted from the received signal in order to produce a new clearer observation for this user. This process may then be iterated. Several studies, e.g., [3] [18], have shown that performance could be increased by using channel coding and performing Soft-Input Soft-Output (SISO) decoding inside each detection iteration. This allows a soft interference cancellation with additional reliability, which reduces the error propagation phenomenon between successive iterations. Alternatively or in conjunction, beamforming antenna arrays [12] may reduce this interference. Recently, several studies have been carried out on the association of IC techniques and antenna arrays for space-time IC [11]. An efficient scheme including beamforming in the soft interference cancellation process has been proposed in [19] assuming perfect channel knowledge. In each iteration, a bank of user-specific space-time (2D) Rake receivers, linearly combining signals from all paths and all antennas, allows additional interference reduction, thus improving the iterative process. To further improve the performance, partial interference cancellation with beamforming has been considered in [13], also in the case of perfect channel knowledge. Actual space-time channel estimation was considered for a comparable iterative space-time soft interference cancellation scheme, where the bank of 2D-Rake receivers is replaced by a linear multi-user detector based on the minimum mean square error (MMSE) criterion [21]. This approach, which requires a matrix inversion with a size proportional to the spreading factor may lead to a non-tolerable increase of computational complexity regarding the large spreading factors allowed in UMTS-FDD systems.

This paper proposes and compares two different iterative pilot-aided space-time soft interference cancellation techniques for unknown channels that are particularly suited to W-CDMA uplink scenarios such as UMTS-FDD. The first approach integrates in the

structure proposed in [19] an explicit space-time channel estimation [5], which is renewed in each iteration to make it benefit from the iterative process. The second approach presents a modification of [19], where a bank of adaptive space-time combiners replaces the bank of 2D-Rake receivers in each iteration. This leads to a complete adaptive iterative space-time soft interference cancellation with no need of space-time channel estimation [16] where, thanks to the iterative process, simple adaptive algorithms can be employed with good convergence properties. Other advantages of our adaptive signal processing technique are its capacity to track short-term space-time channel variations and the insensitivity of the proposed adaptive beamforming to phase array calibration mismatches. Alternatively, iterative space-time interference cancellation with explicit channel estimation is likely to allow an easier implementation by avoiding engineering problems such as the step size optimization according to the transmission conditions.

Both proposed solutions aim at finding the good trade-off between complexity and performance, by including in the iterative process a maximal number of signal processing modules that are required by the receiver, to further improve the detection performance, while keeping the complexity of these modules as low as possible. These studies have been realized in the scope of the IST-1999-10741 ASILUM (Advanced Signal Processing Schemes for Link Capacity Increase in UMTS) project [2], sponsored by the European Commission under the Information Society Technologies (IST) Program. A preliminary evaluation of these techniques has already been presented in parts ([4], [16] and [5]) for conventional uplink W-CDMA scenarios. In this paper, we propose an exhaustive comparative survey of the proposed adaptive and non-adaptive iterative space-time soft interference cancellation techniques and we detail how both techniques can be optimized in a true UMTS-FDD transmission matching 3GPP standard, which implies frame structures with specific data and pilot repartition. For such a system, we show that iterative space-time soft interference cancellation really increases the uplink capacity of UMTS-FDD systems compared with conventional Rake receivers, even when the space and time characteristics of the channel are unknown. Additionally, we propose a complexity analysis and eval-

uate the cost of renewing either space-time channel estimation or adaptive space-time signal processing in every iteration. As far as the capacity increase due to multiple antennas of UMTS-FDD uplink systems is considered, the validity of the space-time channel model used for simulations is of paramount influence for reliable performance evaluation. Therefore, simulations are carried out by using a wideband directional channel model [6] for macro-cellular UMTS environment, which has been validated by measurements. Simulation results show that both schemes are capable to handle very high system loads and to achieve near single-user performance with low pilot power overhead according to the standard. The two iterative approaches experience different behaviors: The adaptive scheme is especially effective in the first iterations whereas the efficiency of the channel estimation-based scheme comparatively increases with the number of iterations.

The remainder of this paper is organized as follows: Section 2 presents the considered UMTS-FDD reference system with detailed description of the transmitter, the wideband directional channel and a conventional 2D-Rake receiver. The FDD frame structure is briefly introduced to describe the different pilot and data configurations that are available in dedicated UMTS-FDD scenarios. Iterative space-time soft interference cancellation is considered in section 3 with a detailed description of the two pilot-aided alternative solutions. Section 4 proposes an evaluation of both receivers' complexity. A performance analysis is presented in section 5 for true UMTS-FDD scenarios allowing a precise evaluation of the capacity increase thanks to the proposed algorithms. The paper is finally concluded in section 6.

2 Reference System Description

2.1 Transmitter

Let us consider the uplink of a UMTS system in FDD mode [1] with K transmitters, the baseband processing units of which are depicted on Fig. 1.

M transport blocks of A information bits are sent for each user k during a Transmission Time Interval of TTI ms. They form the Dedicated Physical Data Channel (DPDCH) of user k. L_p parity check bits are added to each transport block before segmentation into C code blocks. Each code block is encoded by either a convolutional code (with rate 1/2 or 1/3) or a turbo code with rate 1/3. The channel encoding output is a block of N_c coded bits $c_k(i)$, $i = 0, \ldots, N_c - 1$. This coded block is then processed by a user-specific Π_k function, including a radio frame equalization, a first interleaving, a radio frame segmentation, a rate matching and $F = TTI/10$ second interleavings with size $\tilde{N}_c/F$. By adding some padding bits, the radio frame equalization ensures that the block of duration TTI ms can be divided into F frames of 10 ms. The first interleaving changes the position of all N_c bits before their segmentation into $TTI/10$ frames. The rate matching, performing either puncturing or padding, modifies the block size into $\tilde{N}_c/F$ in order that coded bits can be transmitted over 10 ms frames with the available spreading factors $SF = 4$, 8, 16, 32, 64, 128 or 256. The Π_k function outputs a block of $\tilde{N}_c$ interleaved coded bits $\tilde{c}_k(i)$. These data bits are spread by a factor SF into $38400 \times F$ chips with duration 260 ns. Each frame of 38400 chips is segmented into 15 timeslots of 2560 chips.

Besides, for each user k, a Dedicated Physical Control Channel (DPCCH) contains in each timeslot 10 control bits spread by a factor 256. Among them, N_{pilots} bits are pilot bits. Thus, to each data block with size $\tilde{N}_c$, correspond $N_p = F \times 15 \times N_{\text{pilots}}$ pilot bits $p_k(i)$. The timeslot structure is detailed on Fig. 2.

Data bits from DPDCH are modulated in phase with amplitude β_d, whereas control bits from DPCCH are modulated in quadrature with amplitude β_c. After user-specific scrambling, the complex sample $s_k(n)$ of user k at time n is transmitted on the mobile radio channel.

2.2 Wideband Directional Channel

As we intend to apply beamforming at the BS side to increase the performance of UMTS-FDD uplink systems, a space-time channel model which is representative of an actual 2 GHz transmission is needed to get an accurate estimate of the interference mitigation capability of our system. Therefore, we use a Wideband Directional Channel Model (WDCM) [6] that yields a realistic distribution of path Directions of Arrival (DOAs) and delays.

The WDCM, proposed in the IST project ASILUM [14] for micro- and macro-cells, results from a geometrically based single bounce statistical modeling. In this paper, we focus on macro-cells. In this case, clusters of scatterers are uniformely distributed in a circle, the center of which is the Mobile Station (MS). Scatterers have a Gaussian distribution around the cluster's central point and the number of scatterers per cluster follows a Poisson distribution. A complex coefficient, describing the random attenuation and the phase rotation affecting the signal after reflection, is assigned to each scatterer. The model only takes into account the signals from BS to MS experiencing a single reflection. Rough surface scattering, diffraction and multiple reflections are not considered. The amplitude of each signal between MS and BS is computed from the path loss and scatterer's random attenuation. The output of the model is a matrix of complex coefficients associated to different delays and DOAs. The model was assessed by channel measurements [24][14].

The obtained channel for each user k contains P'_k paths, each path p having a delay equal to $\tau_{k,p}$ chips, a complex Gaussian coefficient at time n $h_{k,p}(n)$ with amplitude $\rho_{k,p}(n)$ and phase $\nu_{k,p}(n)$, and a DOA $\theta_{k,p}(n)$. Several paths may have the same delay but different DOAs. We denote P_k the number of distinct delays $\tau_{k,p}$. In the sequel, the channel is assumed stationary over one entire frame in order to simplify the notations but the description can of course be adapted to shorter stationarity periods.

2.3 Two-Dimensional Rake Receiver

Let us now consider the conventional receiver baseband processing unit for the described system. Fig. 3 depicts a space-time combiner (2D-Rake receiver) using a Uniform Linear Array (ULA) with L antennas. Assuming plan wave propagation, the ULA geometry induces a constant additional propagation length from one antenna to the next, equal to $d\cos(\theta_{k,p})$, where d is the distance between antennas. Thus, for DOA $\theta_{k,p}$, the space-time channel coefficient resulting from the specific phase rotation $\phi_{k,\ell,p}$ on antenna ℓ is

$$h_{k,\ell,p} = \rho_{k,p} \exp\left(j\xi_{k,\ell,p}\right) \tag{1}$$

where

$$\begin{aligned} \xi_{k,\ell,p} &= \nu_{k,p} + \phi_{k,\ell,p} = \nu_{k,p} + (\ell-1).\phi_{k,p} \\ &= \nu_{k,p} + 2\pi\frac{d}{\lambda}(\ell-1)\cos(\theta_{k,p}). \end{aligned} \tag{2}$$

λ is the carrier wavelength and $\phi_{k,p}$ is the constant phase rotation between two consecutive antennas. Assuming rectangular pulses and chip-rate sampling at the receiver side, the received sample on each antenna ℓ at time n is

$$\tilde{r}_\ell(n) = \sum_{k=1}^{K}\sum_{p=1}^{P'_k} h_{k,\ell,p}\ s_k(n-\tau_{k,p}) + w_\ell(n) \tag{3}$$

where $w_\ell(n)$ is the Additive White Gaussian Noise (AWGN) on antenna ℓ at time n. For each user k and each path p among the P_k paths with distinct delays, the observation signal on antenna ℓ is handled by two descramblers/despreaders, one for DPDCH and one for DPCCH, each matched to the path delay $\tau_{k,p}$. We obtain from DPDCH complex observations $x^{\text{data}}_{k,\ell,p}(i)$ for $i = 0,\ldots,\tilde{N}_c - 1$, corresponding to the data coded bits $\tilde{c}_k(i)$, and from DPCCH, complex observations $x^{\text{pilot}}_{k,\ell,p}(i)$ for $i = 0,\ldots,N_p - 1$, corresponding to the pilot bits $p_k(i)$. For clarity reasons in the following developments, we use a time-multiplexing between data and pilot observations. We obtain the following $N_D = \tilde{N}_c + N_p$ observations:

$$\begin{aligned} x_{k,\ell,p}(i) &= x^{\text{pilot}}_{k,\ell,p}(i) \qquad \text{for} \quad i = 0,\ldots,N_p-1 \\ x_{k,\ell,p}(i) &= x^{\text{data}}_{k,\ell,p}(i-N_p) \qquad \text{for} \quad i = N_p,\ldots,N_D-1 \end{aligned} \tag{4}$$

corresponding to transmitted bits:

$$\begin{aligned} D_k(i) &= p_k(i) \qquad \text{for} \quad i = 0, \ldots, N_p - 1 \\ D_k(i) &= \tilde{c}_k(i - N_p) \qquad \text{for} \quad i = N_p, \ldots, N_D - 1. \end{aligned} \tag{5}$$

Thanks to the despreading, the observations mainly contain the contribution of a single path. To cancel residual signals in non-desired directions, a beamforming combines signals from the L different antennas. For each antenna ℓ, a single coefficient $\beta_{k,\ell,p}$ is applied since the despread samples are narrow-banded:

$$y_{k,p}(i) = \sum_{\ell=1}^{L} \beta_{k,\ell,p} \; x_{k,\ell,p}(i). \tag{6}$$

Conventional beamforming [12], steering a beam in the direction of the strongest signal, is applied here, i.e., $\beta_{k,\ell,p} = \exp(-j \; \phi_{k,\ell,p})$.

Observations for all paths of user k are then combined using coefficients $\alpha_{k,1}, \ldots, \alpha_{k,P_k}$ to provide us with a single observation $z_k(i)$ for each transmitted bit:

$$z_k(i) = \sum_{p=1}^{P_k} \alpha_{k,p} \; y_{k,p}(i). \tag{7}$$

Maximum Ratio Combining (MRC) is performed here, i.e., $\alpha_{k,p} = \rho_{k,p} \exp(-j \; \nu_{k,p})$.

For each user k, the observations on coded bits are processed by Π_k^{-1}, the inverse of the global framing function Π_k and decoded. Frame error is then tested by using the parity check code.

3 Iterative Space-Time Interference Cancellation

Fig. 4 depicts an iterative space-time interference cancellation receiver with J iterations using a ULA and a SISO decoder, as described in [19], where perfect space-time channel estimation is assumed. In each receiver iteration j, a user-specific multi-antenna observation signal $\tilde{r}_{k,\ell}^{(j)}(n)$, where $\ell = 1, \ldots, L$, provided by the previous iteration $j - 1$, is processed by a space-time combiner as represented on Fig. 3. Note that superscript (j)

is now added to all notations in the sequel. In the first iteration, the observation signal is equal for all users to the received signal:

$$\tilde{r}_{k,\ell}^{(0)}(n) = \tilde{r}_\ell(n), \forall k = 1, \ldots, K. \tag{8}$$

For each user k, the observations on coded bits are processed by Π_k^{-1}, and decoded by a SISO decoder, e.g., a forward-backward decoder, that yields soft estimates $\delta_k^{(j)}(i)$ on coded bits. This stage concludes the detection process of each iteration. Then, the soft estimates are processed by function Π_k. A space-time respreader performs spreading of the Π_k output signal, modulation with reinsertion of DPCCH in the quadrature component, amplitude weighting with coefficients β_d and β_c, scrambling and filtering by the space-time channel impulse response to rebuild each users' contribution in the global interference on each antenna. From these soft contributions, interference cancellation is performed on the received signal to supply the following iteration with a new cleared user-specific observation signal $\tilde{r}_{k,\ell}^{(j+1)}(n)$. Using coded bit estimates after SISO decoding strongly improves the interference cancellation quality, allowing high capacity and near-single-user performance. Note that the last iteration of Fig. 4 only consists in a final detection process without interference cancellation.

3.1 Iterative Space-Time Interference Cancellation with Channel Estimation

As channels are unknown and pilots are available in the UMTS-FDD system, we first propose to include a pilot-aided space-time channel estimation in each space-time combiner, i.e., in each iteration. Since the quality of the observation signal $\tilde{r}_{k,\ell}^{(j)}(n)$ improves from one iteration to the following, the estimation accuracy will also improve, thus making the detection less erroneous. Hence, we expect a performance improvement in comparison with a non-iterative estimation, which would be performed in the first iteration only. Furthermore, since the reliability of coded bit estimates is increased thanks to SISO decoding, the soft values $\delta_k^{(j)}(i)$ of data bits may be used as new pilots in the following iteration for

data-aided estimation. This larger number of pilots for iterations 1 to $J-1$ will further improve the estimation quality and thus the performance.

As done for observations in (4), the $\tilde{N}_c$ soft estimates on coded bits $\delta_k^{(j)}(i)$ are time-multiplexed with the pilot bits:

$$\begin{aligned} \Delta_k^{(j)}(i) &= p_k(i) \qquad \text{for} \quad i = 0, \ldots, N_p - 1 \\ \Delta_k^{(j)}(i) &= \delta_k^{(j)}(i - N_p) \qquad \text{for} \quad i = N_p, \ldots, N_D - 1. \end{aligned} \tag{9}$$

The space-time channel estimation individually computes the complex coefficient and the DOA for each path p of user k, i.e., it works with signals $x_{k,\ell,p}^{(j)}(i)$ for $\ell = 1, \ldots, L$ and $i = 0, \ldots, N^{(j)} - 1$. In iteration 0, the estimation is performed just using pilot symbols ($N^{(0)} = N_p$) whereas coded bit estimates are available to improve estimation in iterations $1, \ldots, J-1$ ($N^{(j)} = N_D$). Two space-time channel estimation algorithms were considered in [5]: A root-MUSIC algorithm with spatial smoothing and a low-complexity estimator based on an approximation of the Maximum Likelihood (ML) criterion, with the restrictive assumption that paths from different DOAs arrive with different delays. Since the former is quite complex and as we aim at performing estimation in each iteration, we focus in this paper on the latter algorithm to limit the receiver complexity. From (3), assuming that the interference from other users and other paths has been perfectly cancelled, we can write the despread signal as

$$x_{k,\ell,p}^{(j)}(i) = h_{k,\ell,p}\, D_k(i) + w'_{k,\ell,p}(i) \tag{10}$$

where $w'_{k,\ell,p}(i)$ is the noise sample on symbol i for antenna ℓ, user k and path p. For a given user and a given path, all noise samples $w'_{k,\ell,p}(i)$, $\forall \ell = 1, \ldots, L$, $\forall i = 0, \ldots, N^{(j)} - 1$, are Gaussian and independent. To perform ML estimation of space-time channel parameters $\rho_{k,p}$, $\nu_{k,p}$ and $\theta_{k,p}$, we must minimize the quadratic Euclidean distance ${d_{k,p}^{(j)}}^2$ between the received sequence and the expected one:

$${d_{k,p}^{(j)}}^2 = \sum_{i=0}^{N^{(j)}-1} \sum_{\ell=1}^{L} |x_{k,\ell,p}^{(j)}(i) - h_{k,\ell,p}\, \Delta_k^{(j-1)}(i)|^2. \tag{11}$$

Note that for iteration 0, $\Delta_k^{(-1)}(i)$ is only composed of pilots since soft estimates $\delta_k^{(-1)}(i)$ are not available. To simplify the minimization, we perform it separately on each antenna to find at iteration j the estimate $\hat{\xi}_{k,\ell,p}^{(j)}$ of the phase rotation $\xi_{k,\ell,p}$ defined in (2):

$$\begin{aligned}\hat{\xi}_{k,\ell,p}^{(j)} &= \arg\min_{\xi}\left(\sum_{i=0}^{N^{(j)}-1}\left| x_{k,\ell,p}^{(j)}(i) - \rho\ e^{j\xi}\Delta_k^{(j-1)}(i)\right|^2\right) \\ &= \arg\left(\boldsymbol{\Delta}_k^{(j-1)^H}\mathbf{x}_{k,\ell,p}^{(j)}\right) \in (-\pi;\pi] \end{aligned} \tag{12}$$

where $\arg(a)$ is the argument of the complex number a and $\mathbf{A}^T$ and $\mathbf{A}^H$ denote the transpose and the transpose-conjugate of $\mathbf{A}$, respectively. Thus, the estimate is the argument of the correlation of the observation sequence $\mathbf{x}_{k,\ell,p}^{(j)} = \left(x_{k,\ell,p}^{(j)}(0),\ldots,x_{k,\ell,p}^{(j)}(N^{(j)}-1)\right)^T$ and the pilot sequence $\boldsymbol{\Delta}_k^{(j-1)} = \left(\Delta_k^{(j-1)}(0),\ldots,\Delta_k^{(j-1)}(N^{(j)}-1)\right)^T$.

Since the antenna array is a ULA, according to (2), the phase rotation $\xi_{k,\ell,p}$, for $\ell = 1,\ldots,L$, is an affine function of the antenna index ℓ. However, the estimate $\hat{\xi}_{k,\ell,p}^{(j)}$ belongs to $(-\pi;\pi]$. Therefore, a phase unwrapping is necessary, which suppresses the effect of the modulo-2π operation. The L obtained phases are corrupted by noise, which is mitigated by a linear regression. This yields the estimates $\hat{\theta}_{k,p}^{(j)}$ and $\hat{\nu}_{k,p}^{(j)}$.
Finally, $\hat{\rho}_{k,p}^{(j)}$ is obtained by minimization of ${d_{k,p}^{(j)}}^2$:

$$\tilde{\rho}_{k,p}^{(j)} = \frac{\sum_{\ell=1}^{L}\Re\left\{e^{-j\ \tilde{\xi}_{k,\ell,p}^{(j)}}\boldsymbol{\Delta}_k^{(j-1)^H}\mathbf{x}_{k,\ell,p}^{(j)}\right\}}{L\ \boldsymbol{\Delta}_k^{(j-1)^H}\boldsymbol{\Delta}_k^{(j-1)}} \tag{13}$$

where $\tilde{\xi}_{k,\ell,p}^{(j)} = \hat{\nu}_{k,p}^{(j)} + 2\pi\frac{d}{\lambda}(\ell-1)\cos\hat{\theta}_{k,p}^{(j)}$ and $\Re\{a\}$ is the real part of a. Right hand side of (13) is the real part of the correlation between the observation sequence and the pilot sequence, after phase correction, averaged over all antennas and normalized by the energy of the pilot sequence. The obtained channel estimates are then employed in the space-time combiner including conventional, i.e., MRC, beamforming and path combining.

3.2 Adaptive and Iterative Space-Time Interference Cancellation

As an alternative to the inclusion of explicit space-time channel estimation in each iteration proposed in section 3.1, we propose here an adaptive space-time signal processing technique to cope with unknown channels with no need of explicit channel estimation. However, in the iterative space-time interference cancellation receiver represented on Fig. 4, both the space-time combiner and the space-time respreader require some knowledge about space-time channel characteristics. Thus, avoiding space-time channel estimation, thanks to adaptive signal processing, impacts both the combining and the respreading techniques.

3.2.1 Adaptive Space-Time Combining

We include in each iteration an adaptive MMSE space-time combiner. Compared with a conventional beamformer, an adaptive MMSE beamformer is able to cancel interfering signals by placing nulls of the antenna diagram in their directions, while pointing its main lobe towards the direction of the desired signal. Furthermore, by contrast with beamforming based on explicit DOA estimation algorithms, adaptive MMSE beamforming can form several lobes towards the different DOAs of an observation signal without any a priori knowledge of the number of DOAs. To ensure a good trade-off between performance and complexity, we choose the Normalized-Least Mean Square (N-LMS) adaptive algorithm [9]. Both disjoint and joint structures have been investigated to perform combining in space and time [23]. We focus on a disjoint adaptive structure, i.e., an adaptive N-LMS beamforming filter followed by an adaptive N-LMS path combining filter. Indeed, dealing with two short filters instead of one larger filter in the joint approach is expected to increase the convergence speed while not inducing too much performance degradation due to the suboptimality of a disjoint process. This results in an adaptive MMSE space-time combining structure represented on Fig. 5, that is related to the conventional structure

depicted on Fig. 3.

After despreading for user k of each path p on each antenna ℓ, the beamformer outputs for each path:

$$y_{k,p}^{(j)}(i) = \boldsymbol{\beta}_{k,p}^{(j)}(i)^T \ \mathbf{x}_{k,p}^{\prime(j)}(i) = \sum_{\ell=1}^{L} \beta_{k,\ell,p}^{(j)}(i) \ x_{k,\ell,p}^{(j)}(i) \tag{14}$$

where $\mathbf{x}_{k,p}^{\prime(j)}(i) = \left(x_{k,1,p}^{(j)}(i), \ldots, x_{k,L,p}^{(j)}(i)\right)^T$ and $\boldsymbol{\beta}_{k,p}^{(j)}(i) = \left(\beta_{k,1,p}^{(j)}(i), \ldots, \beta_{k,L,p}^{(j)}(i)\right)^T$ results from the N-LMS update rule as follows:

$$\boldsymbol{\beta}_{k,p}^{(j)}(i+1) = \boldsymbol{\beta}_{k,p}^{(j)}(i) + \mu_{k,p}^{(j)}(i) \ \epsilon_{k,p}^{(j)}(i) \ \mathbf{x}_{k,p}^{\prime(j)*}(i). \tag{15}$$

$\epsilon_{k,p}^{(j)}(i)$ is the error signal controlling the convergence of the algorithm and $\mu_{k,p}^{(j)}(i)$ is the step size of the N-LMS algorithm [9]. Initialization of vector $\boldsymbol{\beta}_{k,p}^{(0)}(0)$ ensures an omnidirectional beamforming, i.e., $\boldsymbol{\beta}_{k,p}^{(0)}(0) = (L, 0, 0, \ldots, 0)$. A classical way [20] to generate the error signal $\epsilon_{k,p}^{(j)}(i)$ consists in subtracting, prior to path combining, the observation signal, i.e., the beamforming output, from the expected signal, i.e., a pilot weighted by the channel coefficient:

$$\epsilon_{k,p}^{(j)}(i) = \hat{\rho}_{k,p}^{(j)} \ \exp(j\hat{\nu}_{k,p}^{(j)}) \ \Delta_k^{(j-1)}(i) - y_{k,p}^{(j)}(i). \tag{16}$$

Indeed, degradations caused by the multipath channel have not been corrected at this stage of detection process. However, applying (16) would require explicit knowledge of the complex channel attenuation $\hat{\rho}_{k,p}^{(j)} \exp(j\hat{\nu}_{k,p}^{(j)})$, we prefer the following error signal definition avoiding channel estimation:

$$\epsilon_{k,p}^{(j)}(i) = \Delta_k^{(j-1)}(i) - y_{k,p}^{(j)}(i). \tag{17}$$

Since using (17) forces the beamformer to compensate for the channel phase rotation $\nu_{k,p}$, this filtering process may be considered as a *rotated beamforming*.

Then, observations for all paths of user k are combined to provide us with a single observation $z_k^{(j)}(i)$ for each transmitted symbol $D_k(i)$:

$$z_k^{(j)}(i) = \boldsymbol{\alpha}_k^{(j)}(i)^T \mathbf{y}_k^{\prime(j)}(i) = \sum_{p=1}^{P_k} \alpha_{k,p}^{(j)}(i) \ y_{k,p}^{(j)}(i) \tag{18}$$

where $\mathbf{y}_k'^{(j)}(i) = \left(y_{k,1}^{(j)}(i), \ldots, y_{k,P_k}^{(j)}(i)\right)^T$ and the combining coefficient vector $\boldsymbol{\alpha}_k^{(j)}(i) = \left(\alpha_{k,1}^{(j)}(i), \ldots, \alpha_{k,P_k}^{(j)}(i)\right)^T$ is generated from another N-LMS update rule as follows:

$$\boldsymbol{\alpha}_k^{(j)}(i+1) = \boldsymbol{\alpha}_k^{(j)}(i) + \mu_k'^{(j)}(i)\ \epsilon_k'^{(j)}(i)\ \mathbf{y}_k'^{(j)*}(i) \tag{19}$$

where $\epsilon_k'^{(j)}(i)$ is the error signal controlling the convergence and $\mu_k'^{(j)}(i)$ is the step size of the N-LMS algorithm. Initialization of vector $\boldsymbol{\alpha}_k^{(0)}(0)$ ensures an equal gain path-combining, i.e., $\boldsymbol{\alpha}_k^{(0)}(0) = (1, 1, \ldots, 1)$. The error signal $\epsilon_k'^{(j)}(i)$ is generated as:

$$\epsilon_k'^{(j)}(i) = \Delta_k^{(j-1)}(i) - z_k^{(j)}(i). \tag{20}$$

As for our proposed technique based on explicit space-time channel estimation, adaptive algorithms at the first iteration are only processed based on N_p observation signals.

Using the same reference signal in (17) and (20) avoids estimating the channel and enables to jointly optimize the space and time combining filters. Particularly when the structure has converged, the beamforming fully compensates for the channel phase rotation and the path combining only weights each path with a distinct real-valued coefficient. Furthermore, in case of phase array calibration mismatches that may appear during the transmission, our algorithm will also compensate for the corresponding additional phase rotation, which avoids the additional complexity of specific antenna calibration devices.

Besides, channel decoding induces a block-by-block processing of received signals and we assume channel stationarity over one block, e.g., one timeslot or one frame. Thus, at the end of the processing of a given block at iteration j, vectors $\boldsymbol{\alpha}_k^{(j)}(N^{(j)} - 1)$ and $\boldsymbol{\beta}_{k,p}^{(j)}(N^{(j)} - 1)$ are assumed to be closer to the MMSE optimum vectors than the preceding ones. Hence, both final sets of coefficients are re-used to process the same block again, so that the output samples $z_k^{(j)}(i)$ can be generated with additional reliability.

Repeating adaptive space-time combining in each iteration is beneficial for several reasons. On one hand, the reference signal $\Delta_k^{(j-1)}(i)$ can be either a pilot symbol or a self-estimate, which becomes more reliable with the number of iterations. On the other hand, the initialization of adaptive filters for one block at iteration j ($j \neq 0$) is based

on the filter coefficients obtained after the processing of the same block at iteration $j-1$, since these coefficients are expected to be all the closer to the optimum MMSE coefficients as the number of iterations increases. In this way, interference cancellation at iteration j is expected to output a new set of observations $\tilde{r}_{k,\ell}^{(j+1)}(n)$ that are decorrelated from observations $\tilde{r}_{k,\ell}^{(j)}(n)$, at least for the very first iterations, in which the amount of interference is high. The convergence process of the adaptive algorithms can then go on from one iteration to the following one with a lower residual mean square error (MSE). In other words, the iterative process enables to use simple adaptive algorithms, whose low convergence properties are improved thanks to the number of iterations.

3.2.2 Space-Time Respreading

As depicted on Fig. 4, for each iteration, the interference contribution of each user must be regenerated at each antenna connector in order to subtract the space-time interference from the received signal. Thus, the signal estimate $\Delta_k^{(j)}(i)$ of each user must be respread by the associated spreading sequence and filtered by a model of the space-time channel, as represented on Fig. 6.

In order to avoid any explicit estimation of the space-time channel, the interference regeneration process simply uses coefficients issued from the adaptive space-time combining filters. However, since the reference signal is common to both adaptive algorithms, vectors $\boldsymbol{\beta}_{k,p}^{(j)}(i)$ and $\boldsymbol{\alpha}_k^{(j)}(i)$ do not explicitly contain the separated influence of the multi-path channel and DOAs. Therefore, we model the space-time channel in two parts: A path signal regenerator and an antenna signal regenerator. The vector of P_k coefficients $\boldsymbol{\gamma}_k^{(j)}(i)$ used to perform path signal regeneration is derived from the vector of P_k coefficients $\boldsymbol{\alpha}_k^{(j)}(i)$ issued from the path-combining filter as:

$$\boldsymbol{\gamma}_k^{(j)}(i) = \boldsymbol{\alpha}_k^{(j)*}(i). \tag{21}$$

Similarly, the vector of L coefficients $\boldsymbol{\zeta}_{k,p}^{(j)}(i)$ for antenna signal generation relies on vector $\boldsymbol{\beta}_{k,p}^{(j)}(i)$ obtained by the adaptive beamformer. The elements $\zeta_{k,\ell,p}^{(j)}(i)$ of vector $\boldsymbol{\zeta}_{k,p}^{(j)}(i)$

are defined as:

$$\zeta_{k,\ell,p}^{(j)}(i) = \frac{\beta_{k,\ell,p}^{(j)*}(i)}{|\beta_{k,\ell,p}^{(j)}(i)|}. \tag{22}$$

This regeneration process, described by (21) and (22), assumes that the adaptive MMSE space-time combining structure converges to a space-time matched filter as the number of iterations increases. If interference cancellation performs successfully and additive noise is omnidirectional, this condition is valid for an observation signal coming from a single DOA, since MRC and MMSE beamformers have the same antenna diagram. For an observation signal issued from multiple DOAs, this approximation may lead to slight degradations.

4 Complexity evaluation

In this section, the complexity of the proposed iterative receivers is quantified in terms of computational complexity and storage requirements for different UMTS-FDD scenarios [1]: 8 kbps, 64 kbps, 144 kbps and 384 kbps. Note that the 144 kbps scenario, which has been chosen to present performance results, is detailed in the next section.

Algorithms are analyzed based on their respective software implementations for one iteration of the iterative process. The complexity of several iterations may be exactly proportional to the number of iterations or slightly reduced depending on the parallel or cascaded implementation of the whole iterative process. As the processing of the received signal is performed on a slot-by-slot basis, the computational complexity is evaluated for all the functions involved for the detection of one timeslot while the storage requirements depend on the activation rate of these functions (each bit, each slot or each coded block). Besides, all these functions except the interference cancellation block are user-specific. Therefore, results of complexity are presented in the sequel for the detection of one user. Finally, to properly evaluate the impact of multiple antennas on the complexity increase, figures are given as a function of the number of antennas.

In the sequel, for clarity reasons, we will refer to the iterative space-time interference

cancellation using explicit space-time channel estimation as the "non-adaptive" scheme while iterative space-time interference cancellation using adaptive space-time signal processing will be referred to as the "adaptive" scheme. The 2D-Rake receiver with perfect channel estimation ("2D-Rake") will also be considered as a reference.

4.1 Computational complexity

When evaluating the computational complexity, only operations strictly related to the data processing are considered. In other words, operations required for indexing, loop counters, assignments of values to variables, and so on, are not taken into account. Focusing on a fixed point DSP implementation, computational complexity is evaluated in terms of MACs (Multiplications-ACcumulations). Complex additions are approximated to 1 MAC whereas complex multiplications require 4 MACs. Other data processing operations such as division or square root are all estimated at 10 MACs, assuming an iterative implementation.

Table 1 compares for one iteration the computational complexity of the adaptive (resp. non-adaptive) receiver C_{adaptive} (resp. $C_{\text{non-adaptive}}$) to the complexity $C_{\text{2D-Rake}}$ of the 2D-Rake receiver. Decoding is performed by a Viterbi algorithm in the reference 2D-Rake. Then, we can derive the complexity for J iterations ($C^{(J)}_{\text{adaptive}}$ and $C^{(J)}_{\text{non-adaptive}}$) of the proposed techniques as :

$$C^{(J)}_{\text{adaptive}} = (J-1)\, C_{\text{adaptive}} + C_{\text{2D-Rake}} \quad (23)$$

$$C^{(J)}_{\text{non-adaptive}} = (J-1)\, C_{\text{non-adaptive}} + C_{\text{2D-Rake}}. \quad (24)$$

These complexity figures include the complexity of the interference cancellation process. Both proposed iterative receivers induce the same level of complexity whatever the number of antennas and the scenario. In other words, the complexity of our explicit space-time channel estimation is equivalent to the complexity of our adaptive space-time signal processing technique. For the 144 kbps scenario in the single antenna case, the reference receiver has a complexity of 1.4 MegaMAC per user per timeslot. For the same scenario

and $J = 3$ iterations, both proposed receivers induce a complexity of 12 MegaMAC, which is 8.6 times larger. With 4 antennas, the reference receiver has a complexity of 1.8 MegaMAC whereas iterative receivers require 13.6 MegaMAC, which is only 1.1 times the complexity of iterative receivers with a single antenna. Thus, increasing the number of antennas does not impact too much the computational complexity of our systems.

Fig. 7 represents the complexity ratio of the different modules involved in one iteration of space-time interference cancellation for the 144 kbps scenario with 4 antennas. SISO decoding represents 89 % of the overall iteration complexity whereas space-time combining at the chip rate for unknown channels only requires 7 %. In other words, dealing with unknown space-time channels in each iteration by using either explicit space-time channel estimation or adaptive space-time signal processing is reasonable since it does not greatly impact the overall complexity.

4.2 Storage requirements

When evaluating the storage requirements, we enumerate the number of complex values that must be memorized during the activation of each function involved in one iteration. On that basis, it becomes easy to derive the required amount of bytes depending on the implementation choice (float, double, quantized values...).

The storage requirements of the adaptive technique differ in principle from those of the non-adaptive technique. The former consists in the storage of P_k beamforming vectors $\boldsymbol{\beta}_{k,p}^{(j)}$ of size L and a single combining vector $\boldsymbol{\alpha}_k^{(j)}$ of size P_k in order to initialize adaptive algorithms, whereas the latter needs storage of the P_k DOAs $\xi_{k,p}^{(j)}$ and complex signal attenuations $\rho_{k,p}^{(j)} \exp(j\nu_{k,p})$. The storage requirements due to interleaving, deinterleaving, channel decoding and interference cancellation processes are the same for both techniques.

Table 2 compares the storage requirements of the adaptive (resp. non-adaptive) receiver S_{adaptive} (resp. $S_{\text{non-adaptive}}$) for one iteration to the storage requirements $S_{\text{2D-Rake}}$ of the 2D-Rake receiver. Thus, we can derive the storage requirements for J iterations

($S^{(J)}_{\text{adaptive}}$ and $S^{(J)}_{\text{non-adaptive}}$) of the proposed techniques as:

$$S^{(J)}_{\text{adaptive}} = (J-1)\, S_{\text{adaptive}} + S_{IC} + S_{\text{2D-Rake}} \quad (25)$$

$$S^{(J)}_{\text{non-adaptive}} = (J-1)\, S_{\text{non-adaptive}} + S_{IC} + S_{\text{2D-Rake}} \quad (26)$$

where the term S_{IC} results from the storage of initial chip observations needed for the interference cancellation process on the different antennas.

We observe that the difference of storage requirements of the two proposed techniques is negligible with respect to the memory needed by the SISO decoding. Similarly, using a different number of antennas only slightly impacts the total memory requirement. Finally, for the 144 kbps scenario with 4 antennas and 3 detection iterations, the total storage requirement is approximately 7 times the storage needed by the reference 2D-Rake.

5 Simulation Results

In the simulated scenarios, users transmit 144 kbps data in the uplink of the UMTS system in FDD mode. A block ($M = 1$) of $A = 2880$ information bits is transmitted over $F = 2$ frames of 10 ms. $L_p = 16$ parity check bits are added before division into $C = 6$ blocks for rate 1/3 (557,663,711) convolutional encoding. The $N_c = 8838$ coded bits are processed by the Π_k function to provide $\tilde{N}_c = 9600$ bits, which, after spreading in the in-phase signal by a factor $SF = 8$, are transmitted in 2 frames of 38400 chips. In each timeslot, $N_{\text{pilot}} = 6$ pilots among the 10 control bits are spread on the quadrature signal by a factor 256, i.e., $N_p = 180$.

Simulation results are given in terms of Bit-Error-Rate (BER) curves as a function of the signal-to-noise ratio E_b/N_0, where E_b denotes the energy per bit and N_0 the noise spectral density. The $10 \log_{10} L$ dB gain due to multiple antennas justifies the very low E_b/N_0 values. The BER is averaged over all users, who have same power. The 2D-Rake receiver with perfect channel estimation will be considered as a performance reference. In all presented results, the ULA has 4 antennas. DOAs are randomly chosen in a 120 de-

gree sector. For each MT, the WDCM is stationary over 3 timeslots, which results from a mobile velocity around 60 km/h. Both proposed techniques dealing with unknown channels have been presented for a stationarity period equal to one entire frame. They were adapted to a 3 timeslot stationarity period to produce the following results.

5.1 Optimization of pilot energy allocation

According to the UMTS-FDD standard, the power allocated to DPDCH and DPCCH can vary depending on the specified values β_c and β_d. Fig. 8 represents the BER as a function of E_b/N_0 for transmissions with two different DPCCH energies: In Case 1, $\beta_c = \beta_d$ and in Case 2, $\beta_c = 0.2\beta_d$. The non-adaptive iterative detection scheme is applied. As a reference, we also plotted the performance of the 2D-Rake receiver with perfect channel estimation for both allocation cases.

For single-user transmissions, when in-phase (DPDCH) and quadrature (DPCCH) signals have the same amplitude (Case 1), thanks to the high pilot energy as compared to the data energy, the space-time channel estimation is very accurate and 2 iterations are enough to achieve convergence, with a loss of 2 dB as compared to 2D-Rake with perfect estimation. However, the latter performance is quite bad because of the high energy overhead from DPCCH, that dramatically impacts the total transmit power. To really measure the performance improvement brought by our iterative receiver, we simulate a more critical scenario, in which the DPCCH amplitude equals 3/15 of the DPDCH amplitude (Case 2): The power difference between DPDCH and DPCCH equals -14 dB. Since the energy overhead from DPCCH is smaller, the 2D-Rake performance results are improved. Because of the low pilot energy, the first space-time channel estimates provided by our receiver are not sufficiently accurate anymore and a considerable performance loss is observed for iteration 0. This performance loss with respect to the performance of 2D-Rake with perfect estimation is reduced to 2 dB in iteration 4, when channel estimation is performed in each iteration. Due to the difference in DPCCH overhead, we obtain with

our technique a 3 dB gain in Case 2 as compared to Case 1. As this relative behavior is expected to be the same for a higher number of users, we will consider a DPCCH amplitude equal to 3/15 of the DPDCH amplitude in the sequel.

5.2 Influence of the number of iterations

As far as iterative processes are considered, the expected gain in performance provided by each additional iteration must be evaluated to find the good trade-off between performance and complexity. For that purpose, since we aim at dealing with very high system loads, we consider the transmission of 16 users, each following the 144 kbps scenario. Fig. 9 and 10 show the BER averaged over all users versus E_b/N_0 for different number of iterations of the non-adaptive scheme and the adaptive scheme respectively. Both methods are compared to the single-user performance with perfect estimation and the single-user performance when the scheme of interest is applied to cope with the unknown channel.

First, both non-adaptive and adaptive schemes achieve near single-user performance and experience the same general behavior: With the number of iterations, performance increases while the gain provided by each new iteration decreases.

Going into detail, we note that the two proposed techniques exhibit some performance differences. For iteration 4, the non-adaptive scheme only experiences a 1 dB loss (resp. 2.5 dB) with respect to single-user performance with imperfect estimation (resp. perfect estimation) at a BER equal to 10^{-3}. Although the first iteration has promising performance, the adaptive scheme has a stronger loss equal to 3.5 dB for both known and unknown channels, which results from a lack of gain between iterations 2 and 4. Indeed, for the very last iterations, correlation between observations increases, since the residual interference is likely to decrease. Thus, the adaptive MMSE process deals with observations that are strongly correlated with observations provided at the preceding iterations, which reduces the expectable MSE gain from one iteration to the following.

Comparing both techniques on Fig. 11, we see that the adaptive scheme outperforms the non-adaptive scheme for small E_b/N_0 values. Whereas the non-adaptive scheme outperforms the adaptive one for 16 users and low BERs, the opposite behavior is noticed for a single user. Thus, the adaptive scheme is strongly impacted by the multiple access interference. This result contrasts with our expectations based on the two different space-time combining properties: Our 2D-Rake with true channel estimation only copes with the channel of the desired user whereas our adaptive MMSE space-time combiner should have improved the interference mitigation by pointing nulls of the antenna diagram towards undesired directions. In the latter scheme, two reasons can justify this unexpected performance: The convergence of the disjoint adaptive structure based on the N-LMS adaptive algorithm and the assumptions leading to the proposed respreading technique. However, the proposed respreading technique is validated through the performance of the single-user transmission, which shows that adaptive MMSE space-time combining effectively converges to space-time matched filtering. Therefore, reasons of the behavior with multiple users must be found in the low convergence performance of the N-LMS algorithm.

Fig. 11 also represents the performance of other reception techniques: A 2D-Rake with perfect estimation, the non-adaptive scheme using a single antenna with channel estimation performed in every iteration and the non-adaptive scheme using 4 antennas with channel estimation only performed at the first iteration. The 2D-Rake receiver, even with perfect channel knowledge, has very poor performance with an error floor near 10^{-4}. Performance of the non-adaptive scheme using a single antenna are even worst. These results show the advantage of using iterative interference mitigation techniques with antenna arrays. Finally, performance of iterative detection where space-time channel estimation is only performed at the first iteration exhibits a loss of 3.5 dB at a BER equal to 10^{-3} comparing with an iterative process including estimation in each iteration. This confirms the necessity to estimate the unknown channel in every iteration as proposed in this paper.

6 Conclusions

In this paper, we proposed and compared interference mitigation techniques that are particularly adapted to increase the capacity of UMTS-FDD uplink systems. Our iterative schemes, including interference cancellation, beamforming and SISO decoding exhibit near single-user performance for very high system loads, even when space and time characteritics of the channels are unknown. This excellent performance is obtained thanks to the iterative structure of our receivers. We also compared performance of both schemes to more conventional reception techniques such as the 2D-Rake receiver and the iterative receiver with a single antenna, which showed the necessity to envisage advanced detection schemes using antenna arrays in order to cope with highly interfered UMTS-FDD systems. We finally showed that considering the channel as unknown and using several antennas for beamforming in each iteration does not have significant impact on the overall complexity of one iteration.

Acknowledgment

These studies have been sponsored by the European Commission under the Information Society Technologies (IST) Program through the IST-1999-10741 ASILUM project. UMTS simulations have been performed thanks to a transmitter, common to all ASILUM partners. The WDCM was provided by the Instituto Superior Técnico from the Technical University of Lisbon.

References

[1] Third Generation Partnership Project (3GPP), Technical Specification Group Radio Access Network, TS25.211-214 V4.40, available at *http://www.3gpp.org*, Mar. 2002.

[2] IST-1999-10741 ASILUM web site, *http://www.ist-asilum.org*.

[3] L. Brunel, J. Boutros, "Code division multiple access based on independent codes and turbo decoding," *Annales des Télécommunications*, vol. 54, pp. 401-410, Jul./Aug. 1999. Also presented in *Mediterranean Workshop on Coding and Information Integrity*, Ein-Boqeq, Israel, Oct. 1997.

[4] L. Brunel, D. Mottier, "Iterative space-time interference cancellation for W-CDMA systems," *IST-MCS'01*, Barcelona, Spain, Sept. 2001.

[5] L. Brunel, D. Mottier, "Iterative Interference Cancellation Scheme with Pilot-Aided Space-Time Estimation in DS-CDMA Systems," *VTC'01, Fall*, Atlantic City, New Jersey, Vol.1, pp. 197-201, Oct. 2001.

[6] L. Ferreira, M.G. Marques, L.M. Correia, "Implementation of a wideband directional channel model for Link Level Simulations," *IEE Seminar on "MIMO Communication Systems from Concept to Implementation"*, London, UK, Dec. 2001.

[7] V. Ghazi-Moghadam, M. Kaveh, "A CDMA Interference Canceling Receiver with an Adaptive Blind Array," *IEEE Journal on Selected Areas in Communications*, Vol. 16, Oct. 1998.

[8] L.C. Godara, "Application of Antenna Arrays to Mobile Communications, Part2: Beamforming and Direction-of-Arrival Considerations," *Proceedings of IEEE*, Vol. 85, pp. 1195-1245, Aug. 1997.

[9] S. Haykin, *Adaptive Filter theory*. Prentice Hall, 1996.

[10] H. Holma, A. Toskala, *WCDMA for UMTS*. Wiley, 2000.

[11] S. Kapoor, S. Gollamudi, S. Magaraj, Y-F Huang, "Adaptive multiuser detection and beamforming for interference suppression in CDMA mobile radio systems," *IEEE Trans. on Communications*, vol. 48, pp. 1341-1355, Sept. 1999.

[12] H. Krim, M. Viberg, "Two decades of array signal processing research," *IEEE Signal Proc. Mag.*, pp. 67-94, Jul. 1996.

[13] S. Marinkovic, B. Vucetic, A. Ushirokawa, "Space-time iterative and multistage receiver structures for CDMA mobile communication systems," *IEEE Journal on Selected Areas in Communications*, Vol. 19, pp. 1594-1604, Aug. 2001.

[14] G. Marques, J. Pamp *et al.*, "WDCM and measurement campaign," Deliverable 2.3, IST-1999-10741 ASILUM Project, Oct. 2001, *http://www.ist-asilum.org.*

[15] S. Moshavi, "Multi-User Detection for DS-CDMA Communications," *IEEE Communications Magazine*, Vol. 34, pp. 124-136, Oct. 1993.

[16] D. Mottier, L. Brunel, "A low complexity turbo-adaptive interference cancellation using antenna arrays for W-CDMA," *VTC'01, Fall*, Atlantic City, New Jersey, Vol.3, pp. 1644-1648,Oct. 2001.

[17] J.G. Proakis, *Digital Communications, third edition.* New York: McGraw-Hill, 1995.

[18] M.C. Reed, C.B. Schlegel, P.D. Alexander, J.A. Asenstorfer, "Iterative multiuser detection for CDMA with FEC: Near single user performance," *IEEE Trans. on Communications*, vol. 46, pp. 1693-1699, Dec. 1998.

[19] M.C. Reed, P. Alexander, "Iterative multiuser detection using antenna arrays and FEC on multipath channels," *IEEE Journal on Selected Areas in Communications*, vol. 17, pp. 2082-2089, Dec. 1999.

[20] S. Tanaka, M. Sawahashi, F. Adachi, "Pilot Symbol-Assisted Decision-Directed Coherent Adaptive Array Diversity for DS-CDMA Mobile Radio Reverse Link," *IEICE Transactions on Fundamentals*, Vol. E80-A, pp. 2445-2454, Dec. 1997.

[21] J. Thomas, E. Geraniotis, "Soft iterative multisensor multiuser detection in coded dispersive CDMA wireless channels," *IEEE Journal on Selected Areas in Communications*, Vol. 19, pp. 1334-1351, Jul. 2001.

[22] M.K Varanasi, B. Aazhang, "Multistage detection in asynchronous code division multiple access communications," *IEEE Trans. on Communications*, vol. 38, pp. 509-519, Apr. 1990.

[23] X. Wu, A. Haimovich, "Space-time Processing for CDMA Communications," *Proceedings of the 29th Annual Conference on Information Sciences and Systems*, Baltimore, pp. 371-376, Mar. 1995.

[24] E. Zollinger, G. Marques *et al.*, "Wideband directional channel model and measurement campaign," Deliverable 2.1, IST-1999-10741 ASILUM Project, Nov. 2000, *http://www.ist-asilum.org.*

List of Tables

List of Figures

	8 kpbs	64 kbps	144 kbps	384 kbps
$C_{\text{2D-Rake}}$	8.6e4 + 1.2e5 L	5.7e5 + 1.2e5 L	1.3e6 + 1.2e5 L	3.4e6 + 1.2e5 L
$C_{\text{non-adaptive}}$	4.1e5 + 1.7e5 L	2.3e6 + 1.8e5 L	5.1e6 + 2e5 L	1.3e7 + 2.4e5 L
C_{adaptive}	4.0e5 + 1.3e5 L	2.3e6 + 1.4e5 L	5.1e6 + 1.5e5 L	1.4e7 + 1.7e5 L

Table 1: Complexity per user, per iteration and per timeslot for different data rates (L antennas).

	8 kpbs	64 kbps	144 kbps	384 kbps
$S_{\text{2D-Rake}}$	1.23e3	16e3	35.7e3	94.7e3
$S_{\text{non-adaptive}}$	65.8e3	84.3e3	109e3	183e3
S_{adaptive}	66e3 + 0.2e3 L	86e3 + 1.5e3 L	111e3 + 2.9e3 L	188e3 + 5.8e3 L
S_{IC}	2.56e3 L/K	5.12e3 L/K	5.12e3 L/K	5.12e3 L/K

Table 2: Storage per user and per iteration for different data rates (L antennas).

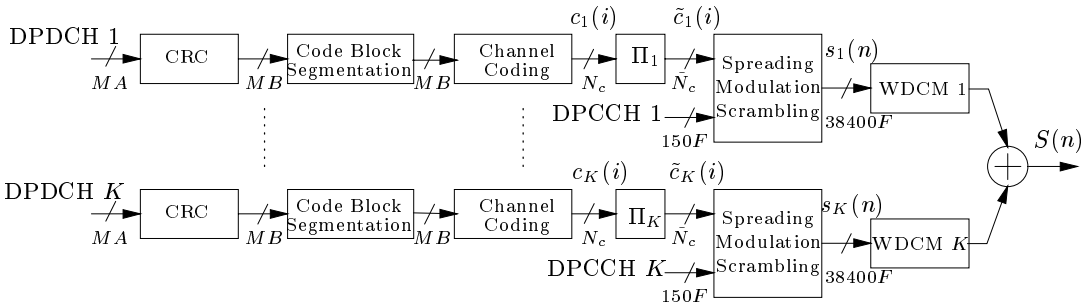

Figure 1: UMTS-FDD transmitter for uplink (K users).

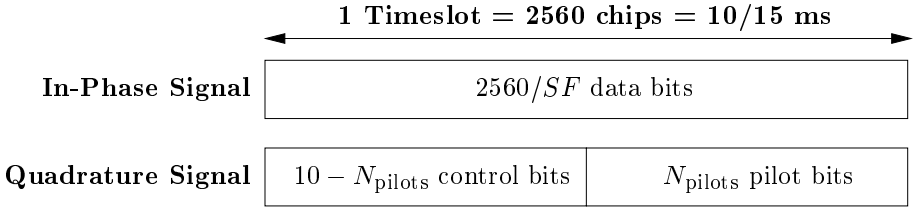

Figure 2: Timeslot structure in UMTS-FDD uplink.

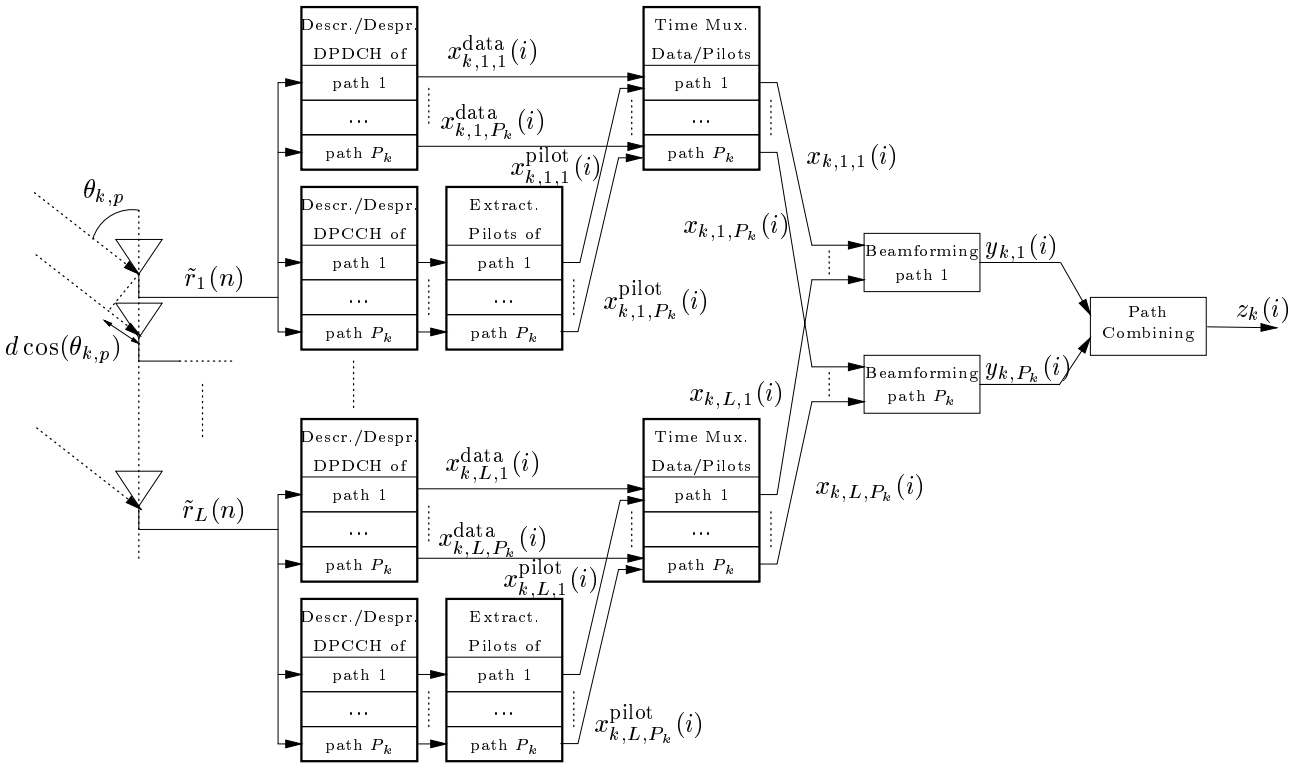

Figure 3: Space-time combiner for user k (L antennas, P_k paths).

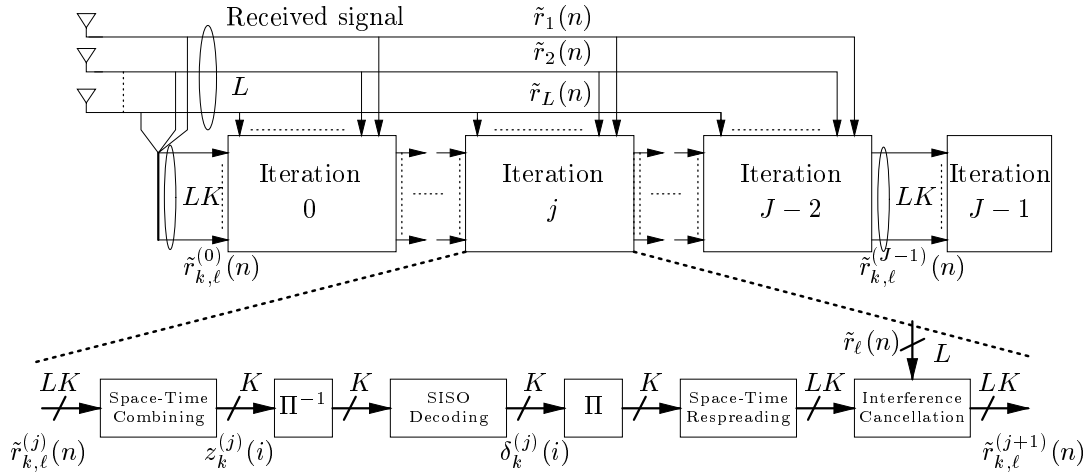

Figure 4: Structure of the iterative space-time interference cancellation receiver (J iterations, L antennas, K users).

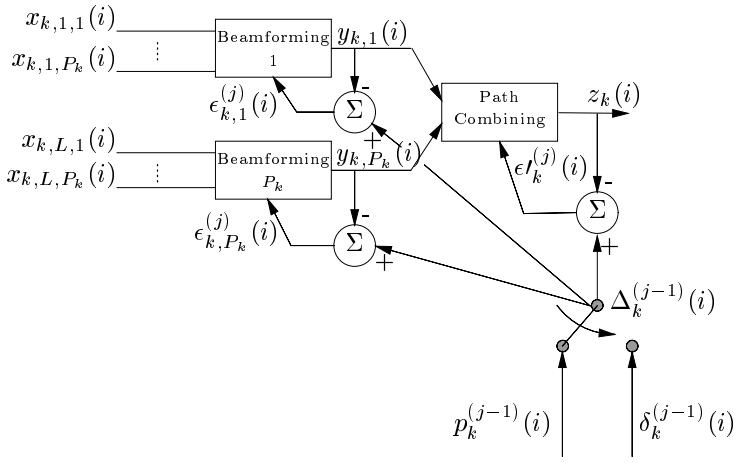

Figure 5: Structure of the adaptive MMSE space-time combiner (L antennas, P_k paths).

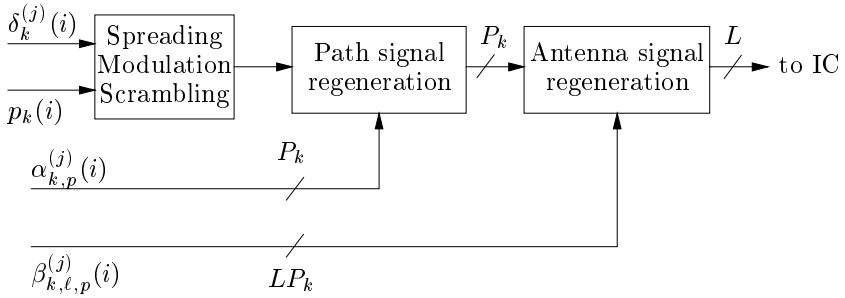

Figure 6: Structure of the space-time respreader (L antennas, P_k paths).

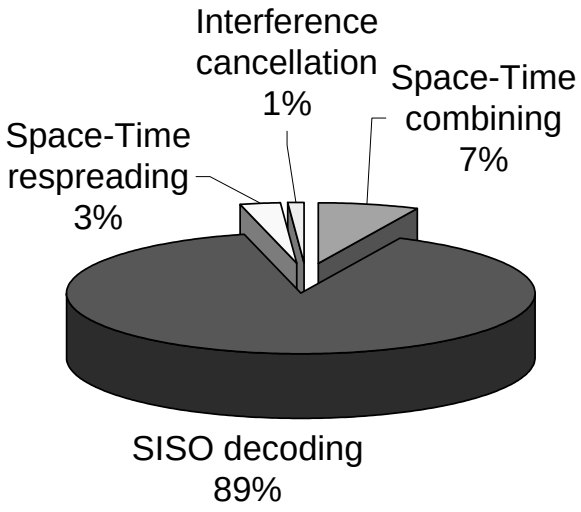

Figure 7: Computational complexity of the different modules in one iteration (144 kbps scenario, 4 antennas).

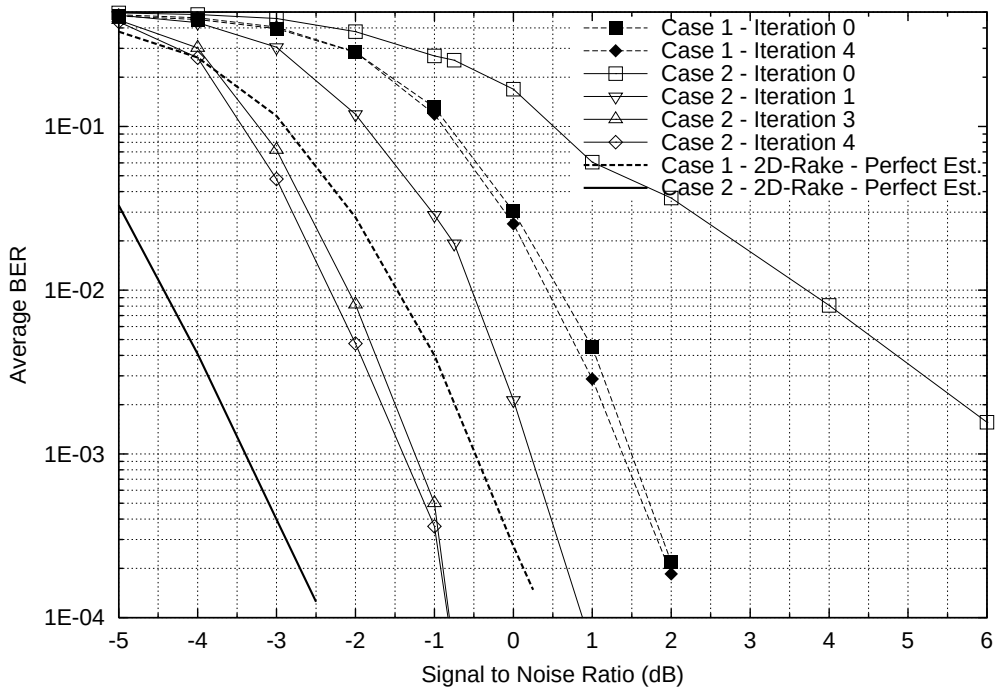

Figure 8: Influence of pilot energy allocation on performance (Case 1: $\beta_c/\beta_d = 1$; Case 2: $\beta_c/\beta_d = 0.2$).

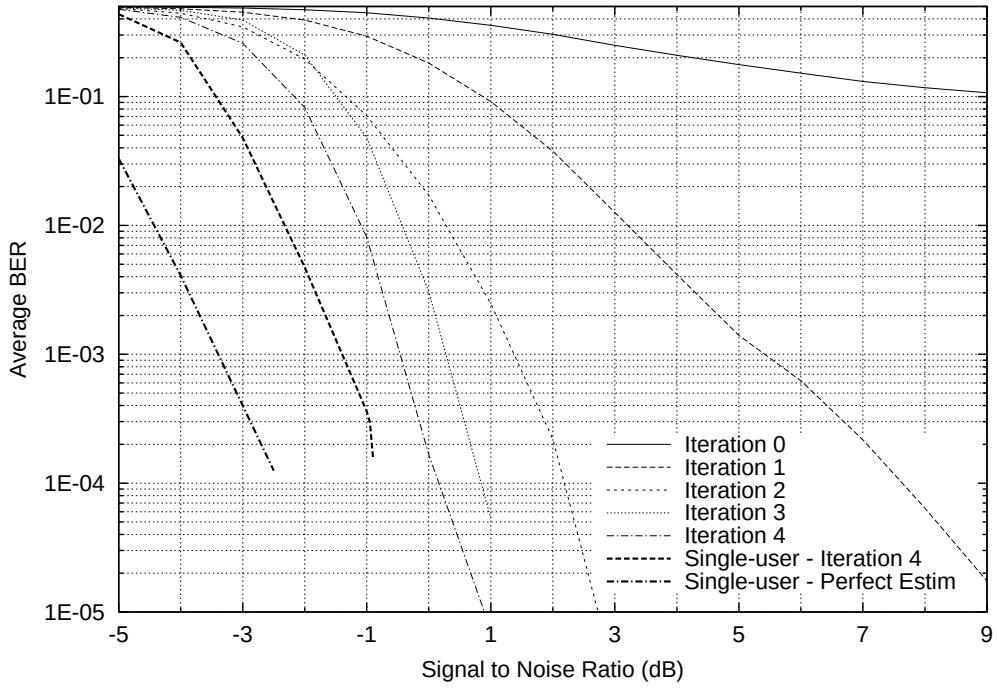

Figure 9: Performance of the non-adaptive scheme (16 users, 4 antennas).

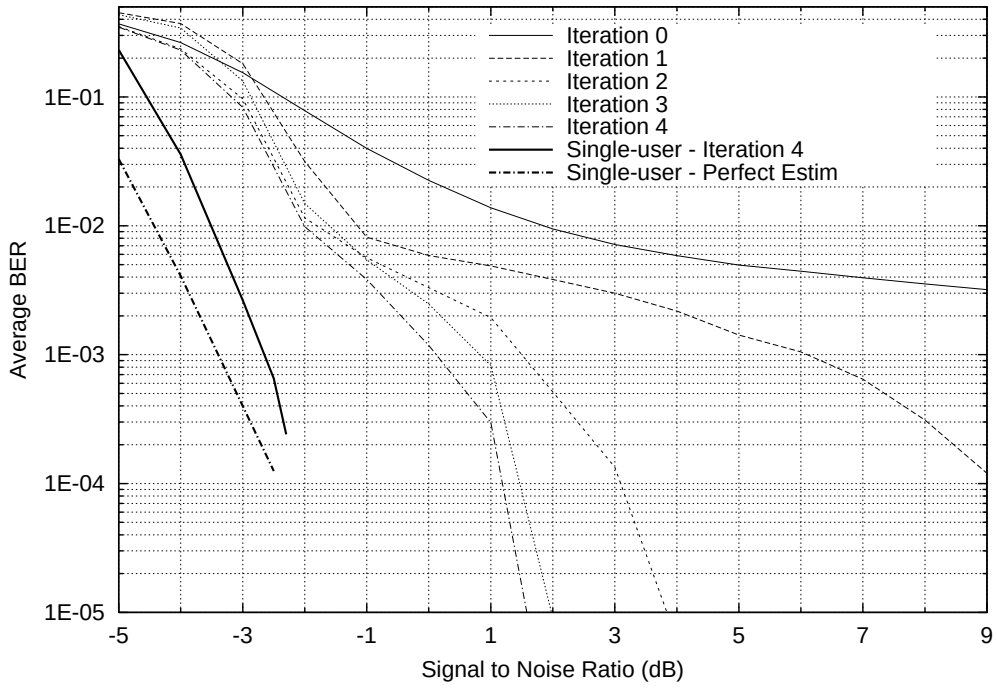

Figure 10: Performance of the adaptive scheme (16 users, 4 antennas).

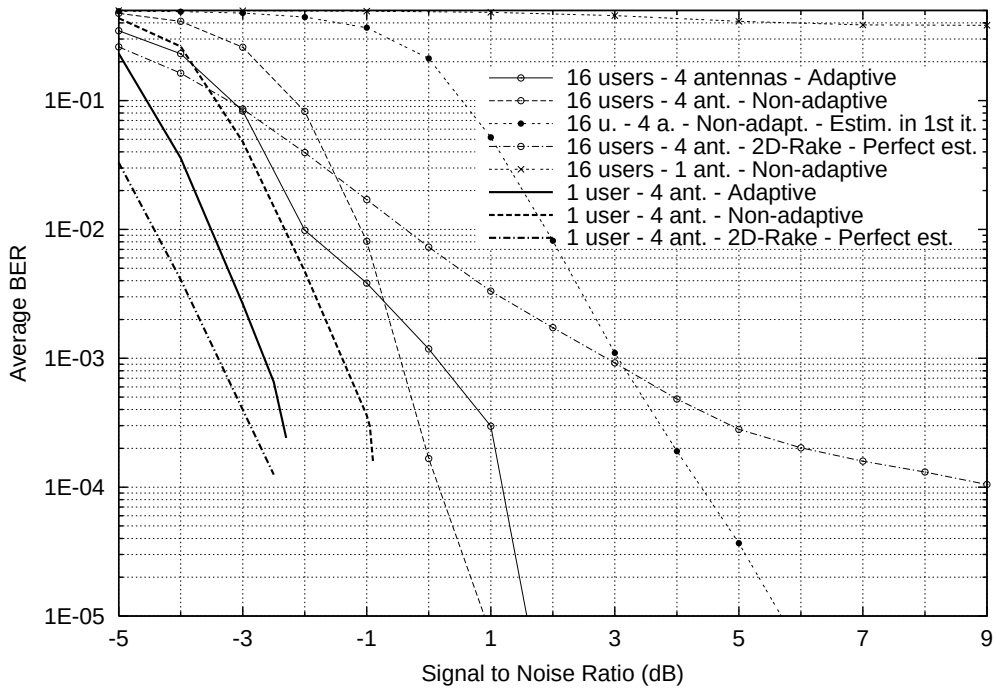

Figure 11: Performance comparison of adaptive and non-adaptive schemes in iteration 4.

Answers to the reviewers' questions

Paper VT-2002-00283

Iterative Space-Time Soft Interference Cancellation for UMTS-FDD Uplink

David MOTTIER - Loïc BRUNEL
Mitsubishi Electric ITE, Telecommunication Laboratory
1, Allée de Beaulieu - CS 10806
35708 Rennes Cedex 7, France
{mottier,brunel}@tcl.ite.mee.com

January 9, 2003
Revision 1.0

REVIEWER 1

- **REVIEWER 1:**

  1) Page 2: The authors mention specifically the high load cases for performance measures. In real life networks the load is never "high". Basically the noise rise (see [10] pages 160 ff the definition) is around 3-6 dB. If the noise rise is more than that, the results tend to be overoptimistic.

  AUTHORS: One objective of introducing multiple antennas in the UMTS system is to increase the system capacity. It is true that real life networks never reach "high" loads because they use low-complexity receiver technologies (Rake receiver, single-antenna). The noise rise approach in [10] is related to these "first-step" receivers. Thus, the 3-6 dB value does not apply in the paper context, since it does not take into account the interference reduction capability of advanced receivers with multiple antennas and multi-user detection.

- **REVIEWER 1:**

  2) Page 5: The high system load is not a reference for performance (see comment 1)

  AUTHORS: See answer to comment 1.

- **REVIEWER 1:**

  3) Page 6: Is the padding bits same as puncturing?

  AUTHORS: No, padding bits are non-informative bits, added to coded bits to obtain a blocksize which is a multiple of $F = TTI/10$. This is done in the radio frame equalisation, which is included in the Π_k function. Rate matching, which is

also included in the Π_k function, performs either padding or puncturing to obtain a spread block which can be transmitted on a 10 ms frame. In contrast to padding, puncturing discards bits. For more details, see reference [1].

To clarify this point, we added in line 10, page 6, "The rate matching, performing either puncturing or padding, modifies...".

- **REVIEWER 1:**

  4) Page 8: $d.\cos(\theta_{k,p})$, there is dot, not a multiplication sign. Should it be changed?

  AUTHORS: For clarity reasons, we deleted all dots.

- **REVIEWER 1:**

  5) Page 8: Actually You have not stated the meaning of the rho in equation (1), although it is quite obvious. But still You should mention it.

  AUTHORS: In page 7, last paragraph of section 2.2, we replaced "$h_{k,p}(n) = \rho_{k,p}(n)\exp(j\nu_{k,p}(n))$" by "$h_{k,p}(n)$ with amplitude $\rho_{k,p}(n)$ and phase $\nu_{k,p}(n)$".

- **REVIEWER 1:**

  6) Page 8: Equation (3): I could not find any statements about the pulse shaping filter, why? This pulse shaping filter is also very important component in receiver side and transmitter side. At least I was expecting a statement that we handle rectangular pulses, thus the pulse shaping is neglected or someting like that.

  AUTHORS: OK, as you proposed, we did the following modification before (3):

"Assuming rectangular pulses and chip-rate sampling at the receiver side, the received sample ...".

- **REVIEWER 1:**

  7) Page 8: You mention that the observation signal on antenna l is filtered by two descramblers. The word "filtered" is quite unusual in this context. I understand the intention, but at least I have found that most of the authors use "multiplied" or "xor" in this context.

  AUTHORS: OK, we replaced "filtered" by "handled".

- **REVIEWER 1:**

  8) Page 9: Again (under equation (6)) there is this dot in $\beta_{k,l,p} = \exp(-j.\phi_{k,l,p})$**. Should it be something else, like multiplication sign?**

  AUTHORS: See answer to comment 4.

- **REVIEWER 1:**

  9) Page 9: Again dot under the equation (7), $\alpha_{k,p} = \rho_{k,p} \exp(-j.\nu_{k,p})$**.**

  AUTHORS: See answer to comment 4.

- **REVIEWER 1:**

  10) Page 9: Have You defined all the variables used in the equations (like ν**)?**

  AUTHORS: $\nu_{k,p}(n)$ is now defined, see answer to comment 5.

- **REVIEWER 1:**

  11) Page 10: You say that You perform the interference cancellation. What exactly You mean by that? Do You subtract respread signal from something or own signal from something? Or do You use some sort of weighting? There is plenty of ways how to perform the IC. Some of them can be numerically unstable.

  AUTHORS: As stated in the paragraph before section 3.1 ("A space-time respreader performs spreading of the Π_k output signal, modulation with reinsertion of DPCCH in the quadrature component, amplitude weighting with coefficients β_d and β_c, scrambling and filtering by the space-time channel impulse response to rebuild each users' contribution in the global interference on each antenna."), interference cancellation is performed at the chip level. Furthermore, we added "soft" in "From these contributions, interference cancellation...", to underline that soft estimates of coded bits are used in the cancellation process.

- **REVIEWER 1:**

  12) Page 12: I did not quite catch how did You end up with equation (12). Could You name the variable $\xi_{k,l,p}$ more accurately than "estimate"?

  AUTHORS: To precise the definition of variable $\xi_{k,l,p}$ we added before equation (12): "to find at iteration j the estimate $\hat{\xi}^{(j)}_{k,\ell,p}$ of the phase rotation $\xi_{k,\ell,p}$ defined in (2)".

- **REVIEWER 1:**

  13) Page 12: Under equation (13): right side $->$ right hand side (add that hand word there)

  AUTHORS: OK.

- **REVIEWER 1:**

  14) Page 13: Last sentence in section 3.2: Commas missing around the "...,thanks to adaptive signal processing impacts,..."

  AUTHORS: OK.

- **REVIEWER 1:**

  15) Page 13: Section 3.2.1. Do You really need commas around "...,i.e.,..."?

  AUTHORS: Yes, according to the English typography and the IEEE guidelines, it seems that these commas are required.

- **REVIEWER 1:**

  16) Page 14: Equation (16). Don't You need absolute value of the error? What does the equation (16) represent? I mean in error terms we usually need absolute values, since error means "how much we are deviating from the correct value".

  AUTHORS: The LMS algorithm requires a signed error signal, see [9] for more details. Roughly speaking, the error sign gives the convergence direction. This error represents the difference between the expected signal and the observed one, both prior to path combining. To clarify this point, we changed the sentence before equation (16) to: "... consists in subtracting, prior to path combining, the observation signal, i.e., the beamforming output, from the expected signal, i.e., a pilot weighted by the channel coefficient."

- **REVIEWER 1:**

  17) Page 14: Equation (17): You use same $\epsilon_{k,p}^{(j)}$ notation for the pilot

aided error as with the original. Should You differiate them somehow, since they are not the same?

AUTHORS: By $\epsilon_{k,p}^{(j)}$, we mean the error signal involved in equation (15), i.e., in the beamforming LMS algorithm, independently of the way it is obtained. For instance, in (20), we used another notation for the error signal of the other LMS algorithm, the path combining one. Therefore, we prefer not modifying the notation.

- **REVIEWER 1:**

18) Page 14: Is there any numerical problems related to the definition of equation (17)?

AUTHORS: Modifying the error signal as done in (17) does not impact the stability. Indeed, from the beamforming point of view, changing the reference signal only changes the phase of the obtained beamformer. Besides, using the same pilot symbol $\Delta_k^{(j-1)}(i)$ in the beamforming and path combining LMS algorithms, ensures a convergence of both filters through the same direction, avoiding the "ping-pong" effect.

- **REVIEWER 1:**

19) Page 18: About the complexity, the authors have chosen the MAC approach. From the practical point of view I would say that it is feasible if we consider DSP's, since in DSP we can do one multiplication and one summing in one clock cycle. But from ASIC point of view the it's not feasible, since we need more circuits to perform the multiplication than the summing.

AUTHORS: Implementation work in our research center is mainly based on fixed point DSPs. This is the reason why we expressed the complexity in terms of MACs.

To clarify this point, we added in the third sentence of section 4.1:

"Focusing on a fixed point DSP implementation."

- **REVIEWER 1:**

  20) Page 18: Isn't the division complexity related to the word length? I mean that You do the division is some table based method, where the complexity is depending about how big is the word? Do You refer to 8 bits word?

  AUTHORS: For the 10 MAC approximation (division and square root), we based our thinking on an iterative algorithm (e.g., CORDIC), where the number of iterations is roughly equal to the required precision, i.e., the word length. We approximated one iteration to one MAC.

  To precise it, we added at the end of the first paragraph of section 4.1:

  "assuming an iterative implementation."

- **REVIEWER 1:**

  21) Page 18: Why You have estimated the division and square root to be 2.5 times more complex than the multiplication and 10 times more complex than adding? I would like to know the reasoning.

  AUTHORS: See answer to comment 20.

- **REVIEWER 1:**

  22) Page 18: In equations (23) and (22) there is the dots. See e.g. comment 8.

  AUTHORS: See answer to comment 4.

- **REVIEWER 1:**

  23) Page 19: Do You need the comma after word Thus below equation (25)?

  AUTHORS: Yes, comma is often used after "Thus".

- **REVIEWER 1:**

  24) Page 20: In the results You plot BER = 10E-5, which means that You need at least 10E6 bits to be simulated, supposing that You need to generate 100 errors in the simulation in order that the simulation is statistically correct (this is a rule of thumb). So how many bits/frames You have simulated totally? This is very important issue here.

  AUTHORS: We simulated 150 frames, i.e., 216000 information bits per user. As we averaged the BER over 16 users, it was computed on 3456000 information bits. Thus, the results given for BER=10^{-5} rely on more than 300 errors.

- **REVIEWER 1:**

  25) Page 29: Figure 4. There is L.K. Should it be L*K?

  AUTHORS: OK.

REVIEWER 2

- **REVIEWER 2:**

  Comments for Author: A result showing where the " MRC == MMSE under ideal IC " assumption is not true would be interesting. Or, when the receiver fails is this the failure mode?

  AUTHORS: In the WDCM model we used, it may occur that several paths have the same delay with distinct DOAs. Thus, the hypothesis that the LMS algorithm converges to the MRC solution is not always true. In this case, the respreading is sub-optimal as mentioned in the sentence before section 4. Simulation results include the impact of this sub-optimality.

- **REVIEWER 2:**

  Does the complexity analysis include the IC block? Shouldn't IC block complexity scale with K since you are adding K signals?

  AUTHORS: Yes, the complexity analysis includes the IC block. As this complexity is expressed on a per user basis, the number of users K does not appear in table 1. However, as the storage of the received signal is common to all users and all iterations, we had to express it separately in table 2. This is inversely proportional to K, since the storage is also given on a per user basis.

  To point out that the IC complexity is including in equations (23) and (24), we added after equation (24): "These complexity figures include the complexity of the interference cancellation process."

REVIEWER 3

- **REVIEWER 3:**

  Comments for Author: Minor changes only are needed :

  - please specify the criterion used to distinguish "distinct" path delays in the multipath WDCM, i.e. to pass from P'_k to P_k

  AUTHORS: In the paper, we do not consider oversampling. Thus, resolvable paths have delays expressed in chip durations. As delay for path p of user k is $\tau_{k,p}$ chips, by distinct delays, we mean distinct values of $\tau_{k,p}$.

  To clarify it, we replaced "with distinct delays" by "with distinct delays $\tau_{k,p}$".

- **REVIEWER 3:**

  - in equation (6) the index l goes from l=1 (not l-1) to l=L

  AUTHORS: This seems to be a printer failure. We did not observe this error on our hard copies.

- **REVIEWER 3:**

  - please expand a bit the explanation of equation (13), i.e. phase unwrapping followed by a linear regression.

  AUTHORS: To clarify this point, we modified the paragraph preceding equation (13) as follows:

  "Since the antenna array is a ULA, according to (2), the phase rotation $\xi_{k,\ell,p}$, for $\ell = 1, \ldots, L$, is an affine function of the antenna index ℓ. However, the estimate $\hat{\xi}^{(j)}_{k,\ell,p}$ belongs to $(-\pi; \pi]$. Therefore, a phase unwrapping is necessary, which suppresses

the effect of the modulo-2π operation. The L obtained phases are corrupted by noise, which is mitigated by a linear regression. This yields the estimates $\hat{\theta}_{k,p}^{(j)}$ and $\hat{\nu}_{k,p}^{(j)}$.

Finally, $\hat{\rho}_{k,p}^{(j)}$ is obtained by minimization of ${d_{k,p}^{(j)}}^2$:"

- **REVIEWER 3:**

  - Fig. 1 bigger if possible

  AUTHORS: OK. In the new version, we drew Fig. 1 as big as possible.

- **REVIEWER 3:**

  - Simulations : what about scenarios with users transmitting at different rates and/or with different powers (no power control)? is BER affected in this case by number of antennas, number of iterations and pilot energy allocation ? what about more than 4 BS antennas and higher-speed MSs?

  AUTHORS: The main objective of the paper is to compare adaptive and non-adaptive space-time techniques in an interference cancellation structure. There are a lot of parameters in the system. We chose a specific scenario and presented results for 1 and 16 users and 1 and 4 antennas. The paper already includes 4 simulation results' figures. Presenting additional results, with different user amplitudes, different number of antennas, pilot energies, data rates, would lead, from our point of view, to similar results and redondant figures.